Science in China Series D: Earth Sciences

www.scichina.com
earth.scichina.com
www.springerlink.com

Reconstruction of the western Pacific warm pool SST since 1644 AD and its relation to precipitation over East China

ZHANG ZiYin†, GONG DaoYi, HE XueZhao, GUO Dong & FENG ShengHui

State Key Laboratory of Earth Surface Processes and Resource Ecology, College of Resources Science and Technology, Beijing Normal University, Beijing 100875, China

Based on coral proxies we reconstructed the western Pacific warm pool sea surface temperature (SST) since 1644 AD. High-frequency reconstructions are based on eight high-pass filtered coral series and raw reconstructions are derived from eight unfiltered coral series, respectively. Validation and comparison with other SST/temperature series show that the reconstructed warm pool SST is highly reliable. The leading periods of warm pool SST are ~2.1, ~2.3, ~2.9, ~3.6, ~3.8, and 80.7-year during the last ~360 years. The warm pool SST exhibits some obvious long-term trends: an upward trend of 0.04℃ per century for the period of 1644—1825, while a decreasing trend of 0.24℃ per century for the period of 1826—1885, and then a remarkable warming trend of 0.28℃ per century taking place between 1886 and 2006. Especially, the SST shows the strongest trend of 0.67℃ increase per century during the last 50 years, a warming unprecedented since 1644 AD. On interannual timescale, the connections between ENSO and the warm pool SST are robust during the reconstruction period. There are significant correlations between the warm pool SST and summer precipitation of the Yellow River basin and Huaihe River basin; the correlation coefficients are –0.44 in reconstruction period (1880—1949 AD) and –0.46 in instrumental period (1950—2005 AD) respectively. This relationship is also found between flood-drought index and the warm pool SST during the past 360 years, and their correlation coefficients are –0.20 in reconstruction period and –0.46 in instrumental period respectively, significant at the 0.01 level. On interdecadal timescale, this connection is more robust, and the correlation coefficient of the low-pass filtered components is –0.42 during the whole period (1644—2000 AD). When the warm pool is warmer than normal, the precipitation is usually below the normal in the Yellow River and Huaihe River basin. On the contrary, when the warm pool is colder than the normal, there may be more precipitation. The reconstructed warm pool SSTs provide useful information and reference for further research on climate change mechanism in East China.

western Pacific warm pool, coral, reconstruct, sea surface temperature

The tropical western Pacific, with the highest sea surface temperature (SST) and the largest warm water bodies on the earth, is the so-called tropical western Pacific warm pool. The thermal state of warm pool has important influences on East Asian monsoon and ENSO system, and it is a key factor of the climate variability in East Asia[1−3]. Due to the lack of sea temperature observation, the studies of the SST variations of the past several centuries, especially the low-frequency variations and its influences upon climate changes in China, are seriously obstructed. Since Knutson[4] used coral to study the sea

Received March 22, 2008; accepted September 16, 2008
doi: 10.1007/s11430-009-0140-x
†Corresponding author (email: zzy@ires.cn)
Supported by National Key Technology Research and Development Program (Grant No. 2007BAC29B02) and Special Fund for Public Welfare Industry (Meteorology, Grant No. GYHY200706010)

Citation: Zhang Z Y, Gong D Y, He X Z, et al. Reconstruction of the western Pacific warm pool SST since 1644 AD and its relation to precipitation over East China. Sci China Ser D-Earth Sci, 2009, 52(9): 1436-1446, doi: 10.1007/s11430-009-0140-x

climate environment, the application of coral has widely developed[5−15], and the coral proxies have been widely used to reconstruct the past SST, rainfall or local runoffs. But most of these works used single coral proxy to analyze the change of local climate elements. In recent years, Evans et al.[16] reconstructed the whole Pacific sea surface temperature field from multiple coral $\delta^{18}O$ data using reduced space objective analysis, and Wilson et al.[17] used the multiple coral proxies to reconstruct the temperature changes of the whole tropical sea area. These works provided a new methodology for the SST reconstruction research. This paper is trying to use the available coral proxies to reconstruct the strength index of the tropical western Pacific warm pool back to 1644 AD, and discuss the relationship between the variability of warm pool SST and climate changes in China.

1 Data and methods

1.1 Research area

Different definitions of the western Pacific warm pool are used in previous studies. Some authors defined the warm pool as the mean SST averaged over a region confined by certain latitudes and longitudes[18−22], some authors defined it as the extent enclosed by a certain SST isoline (see, 28℃, 28.5℃ or 29℃)[7,23−27], and some studies used warm water volume to define the warm pool[28]. To emphasize the main body of the warm water, here we define the warm pool SST as the mean SST in 30°N−30°S and 100°E−140°W where annual SST is above 28℃ (Figure 1). The mean SST in this region is used as the warm pool temperature index, and the sum of the grid number in this region is used as the warm pool area index. Correlation coefficient between the temperature index and the area index is +0.88 during the 1950−2006 time period, significant at the 0.01 level. This indicates that the warm pool area is in good agreement with the warm pool temperature variation, and a higher SST tends to be accompanied by expansion of warm water extent. Thus, in the present study we selected the warm pool's mean SST as the target for reconstruction.

The mean annual warm pool SST is 28.94℃ from 1950 to 2006. The main body of the warm pool lies in the tropical region near the equator and is affected by the land-sea distribution and the seasonal precipitation, with obvious seasonal cycles. The high SST appears in April, May and June and the maximum exists in May. Here, we take the relatively warm March−July as target months for SST reconstruction.

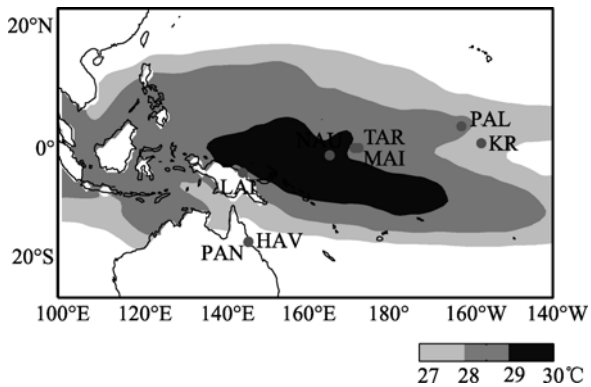

Figure 1 Research area and coral proxy sites. See Table 1 for details of the coral information.

1.2 SST data

The observation SST data (HadISST) used to calibrate in reconstruction are obtained from British Met Office Hadley center. HadISST data sets began in 1871, with monthly temporal resolution and 1°×1° spatial resolution. There are interpolating errors in many regions during the early periods when instrumental records are very sparse, and the errors are minimum after 1950 in most part of the interpolated regions[29,30]. So, we select the HadISST data since 1950 as the observational sea surface temperature for computing the warm pool index.

1.3 Coral proxy data

There are 16 coral proxies available in the western Pacific, which lie mainly in the warm pool and its adjacent area. There exist universally low-frequency variations in climate time series; this may result in spurious high correlation between two indexes with no physical link. In order to reduce the impact of coral proxy low-frequency variations on the reconstructions, we excluded the fictitious information contained in coral proxies. Thus, we first check the high-frequency variability. If the high-frequency variations of coral proxy are related significantly to the warm pool SST with clear physical meaning, then we further check the low-frequency. Only coral proxies significantly correlated with warm pool SST on both high- and low-frequency timescales are selected as potential predictors for reconstruction. Thus, our approach is first to check the high-frequency components (<10 a) for each coral proxy time series using a Butterworth filter, and then to calculate the correlation

Table 1 List of proxy data[a)]

No.	Coral site	Time interval (AD)	Resolution	Type	Latitude	Longitude	Reference
1	HAV (Havannah)	1644－1986	Y	Flu	18.41°S	146.33°E	Isdale et al.[5]
2	PAN(Pandora)	1737－1980	Y	Flu	18.49°S	146.26°E	Isdale et al.[5]
3	MAI(Maiana)	1840－1994	B	δ^{18}O	1°N	173°E	Urban et al.[6]
4	LAI(Laing)	1885－1992	Q	δ^{18}O	4.15°S	144.88°E	Tudhope et al.[7]
5	PAL(Palmyra)	1886－1998	M	δ^{18}O	5.52°N	162.08°W	Cobb et al.[8]
6	NAU(Nauru)	1892－1994	Q	δ^{18}O	0.5°S	166°E	Guilderson et al.[10]
7	TAR(Tarawa)	1894－1989	M	δ^{18}O	1°N	172°E	Cole et al.[11]
8	KIR(Kiritimati)	1939－1993	M	δ^{18}O	2.0°N	157.3°W	Evans et al.[12]

a) Y, yearly; Q, quarterly; M, monthly; B, bi-monthly; Flu for coral Fluorescence.

coefficient of the high- and low-frequency components with the warm pool SST series. When the best representative coral proxies with optimal period (months or seasons) are identified, we used them to reconstruct the warm pool SST. Because coral usually lives in 10－30 m depth under surface water, there may be some time-lags for coral proxies in responding to sea surface temperature variations [31]. After the screening procedures, eight coral proxies were finally selected for reconstruction (see Table 1). Statistical indices show that the high-frequency correlations between the coral proxies and the warm pool SST in calibration period range from –0.39 to –0.58, with a mean value of –0.47, all significant at the 0.05 level. The correlations for the un-filtered raw data range from –0.24 to –0.61, with a mean value of –0.51, all significant at 0.05 level except for KIR of which it is significant at the 0.10 level (Table 2).

Table 2 Correlation (r) between March to July mean warm pool SST and coral proxies within calibration period (1950－1980)[a)]

Proxy	r_1	r_2	Proxy season
HAV	–0.43*	–0.52**	—
PAN	–0.50**	–0.51**	—
MAI	–0.58**	–0.60**	Mar－Jun
LAI	–0.39*	–0.42*	Jul－Dec
PAL	–0.48**	–0.59**	Mar－May
NAU	–0.53**	–0.61**	Apr－Jun
TAR	–0.48**	–0.56*	Mar－May
KIR	–0.40*	–0.24	Jul－Oct
Mean	–0.47	–0.51	

a) *, significant at the 0.05 level; **, at the 0.01 level; pearson correlation 2-tailed test. —, yearly resolution. r_1, r between coral proxies and high-pass filtered data; r_2, r between coral proxies and un-filtered data.

The selected eight coral proxies from published works are shown in Figure 1 and Table 1, of which HAV and PAN are coral fluorescence and the other six proxies are coral stable isotope (δ^{18}O). Coral oxygen isotopes are a robust recorder of environmental variables. Coral δ^{18}O faithfully records interannual variability even when strongly influenced by kinetic effects[10]. Although coral δ^{18}O are affected by both temperature and precipitation[32], given the high correlation between rainfall and temperature over the western Pacific warm pool[7], the coral δ^{18}O could also reflect sea temperature variations in general. Isdale at al.[5] used coral fluorescence proxies taken from Havannah island and Pandora island to reconstruct runoff and precipitation changes in tropical area. Because rainfalls in tropical Ocean come mainly from convective activity, the high temperature is beneficial to ascending motion by the heating effect, resulting in more rainfall and runoff through the more convective activities. Thus, coral fluorescence has also been used to explain the changes of temperature[17]. It is worth noting that HAV and PAN, MAI and TAR records come from almost the same location (Figure 1). Therefore, taking a simple average of all the coral records would result in a bias to this location as it is effectively sampled twice. To remove this bias, we combined the four records into two composites called HPA and MTA respectively. Because the range and variance of HAV and PAN are similar at the same period (1737－1980 AD), we took a simple average of HAV and PAN to get a series called HPA. Contrarily, the range and variance of MAI and TAR are obviously different, and therefore we standardized them first, and then the normalized time series are averaged to yield MTA.

1.4 Reconstruction methods, calibration and verification

Based on the eight selected coral proxies, the warm pool SST-proxy relations were calibrated and cross-validated for the period of 1950－1980. These procedures are performed by applying multivariate regression method, using the raw data of all eight proxies (designed for the low-frequency components reconstruction) and the high-pass filtered data of all eight corals (designed for high-frequency reconstruction), respectively. Then re-

gressions were employed to compute the warm pool SST in 1644－1949. In verification procedure, we checked the explained variance (r^2), standard error (SE), and the reduction of error (RE). The cross-validation was performed by applying a leave-one-out validation method[17,31]. The RE statistic was first described by Lorenz[33] as a way of determining if a meteorological forecast was better than climatology (i.e., the mean of the meteorological data in the calibration period). Then RE was widely used in regression reconstruction of climates[17,34−36]. Fritts[34] noted that RE is an extremely rigorous verification statistic because it has no lower bound, which ranges from +1.0 to −∞. RE>0 indicates reconstruction is skillful, RE>0.2 indicates reconstruction is reliable, and RE=1.0 indicates perfect estimation.

2 Results and discussion

Reconstructions are shown in Figure 2. For raw-reconstruction, the explained variance of the warm pool SST increases from 27% in 1644－1736 when only one predictor is used up to 68% in the recent period when all eight coral proxies are included, with an average of 55%. During period 1644－1949 the explained variance remains relatively stable with an average of approximately 55% (Table 3). At the same time the SE, calculated based on the unresolved variance in the calibration period, varies little with time (0.071－0.096℃). The RE changes from +0.18 to +0.46 with an average of approximately 0.34. To include more skillful proxies would be helpful to reduce the uncertainties in the

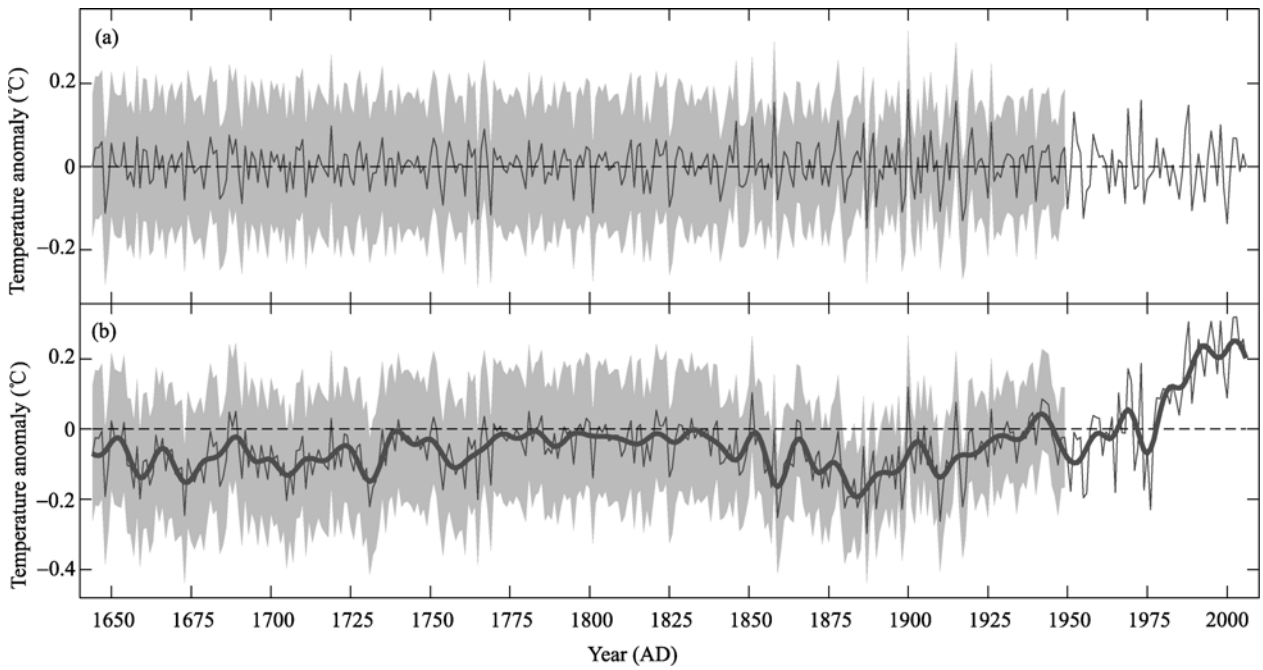

Figure 2 Reconstructed warm pool SST given as anomalies (in ℃, w.r.t. 1971－2000). (a) The high-frequency reconstruction derived from eight filtered coral proxies; (b) the raw-reconstruction based on eight unfiltered coral proxies, and smooth line is the low-frequency (>10 a) variations from a Butterworth filter. Shading indicates the range of ±2×SE derived from unresolved variance in the calibration period.

Table 3 Statistics for the calibration and verification

Proxy number	Period	High-frequency reconstruction			Raw reconstruction		
		r^2 (%)	SE (℃)	RE	r^2 (%)	SE (℃)	RE
8	1938－1949	59	0.070	0.23	68	0.071	0.35
7	1894－1937	58	0.071	0.20	67	0.072	0.33
6	1892－1893	56	0.068	0.26	67	0.072	0.33
5	1886－1891	55	0.067	0.33	65	0.071	0.46
4	1884－1885	53	0.068	0.35	60	0.074	0.45
3	1840－1883	43	0.073	0.32	52	0.079	0.44
2	1737－1839	26	0.082	0.16	31	0.094	0.21
1	1644－1736	19	0.086	0.09	27	0.096	0.18
Mean		46	0.073	0.24	55	0.079	0.34

raw-reconstruction in any future study. Generally, the positive RE values are indicative of reliable reconstruction. For the high-frequency reconstruction, the explained variance of the warm pool SST increases from 19% up to 59% with an average of 46%. Also, the RE changes between +0.09—+0.35. These statistics indicate that both raw and high-frequency reconstructions point to relatively skillful estimates for approximately the last 360 years.

The raw-reconstruction shows a linear trend of +0.04 ℃/100 a for the period of 1644—2006, significant at the 0.01 level. With respect to the trends, three stages can be found: the first is 1644—1825, with a significant trend of +0.04 ℃/100 a; the second is 1826—1885 with a significant trend of –0.24 ℃/100 a; and the third is 1886—2006 with a significant trend of +0.28 ℃/100 a. A rapid temperature increase since 1950 with a linear trend of 0.67℃/100 a is unprecedented during the last 360 years. In addition to the trends, the raw-reconstructions show obvious decadal variations before 1770s, then it fluctuated weakly until 1840s, and then it had significant decadal variations again with strong warming trend since 1840s. This feature in reconstructed warm pool SST is comparable with the another SST series as presented by Zhou at al.[37] during the 1871—1997 period, especially on interdecadal timescale, e.g., the same low temperature during 1870s—1930s, the same fluctuating with a stable warming trend since 1950s. To check more details of the periodicity, we performed the power spectral analysis. The results indicate that the leading periods of the warm pool SST are ~2.1, ~2.3, ~2.9, ~3.6, ~3.8, and ~80.7-year during the last 360 years (Figure 3). And the periods of ~5.4, ~7.1-year are also relatively outstanding. Same analyses for different sub-time periods show that the 2—4 year variations are the most stable high- frequency through the whole 360 years period.

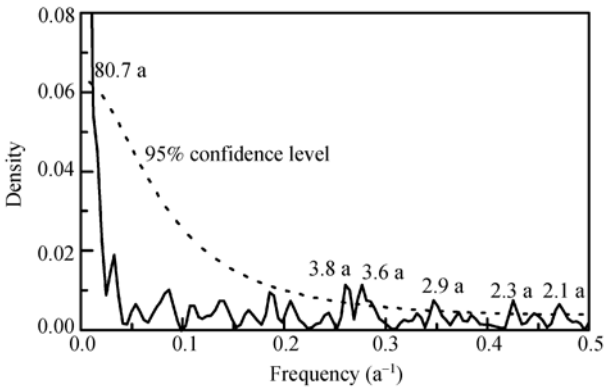

Figure 3 Power spectral analyses for warm pool SST.

The leading high-frequency periodicities of the warm pool SST are similar to El Niño-Southern Oscillation (ENSO) frequency feature[38], indicating the variability of the warm pool SST may be connected with ENSO. Comparison of the high-frequency reconstruction SST and SOI (there the SOI is defined as the air pressure differences between Tahiti and Darwin, and the monthly data are obtained from Australian Bureau of Meteorology, website: http://www.bom.gov.au/climate/current/soihtm1.shtml) is shown in Figure 4, where SST for the 1950—2002 period is from the observational SST and the reconstructions are shown for the 1876—1949. There are significant negative correlations between the mean warm pool SST (March to July) and the mean SOI from preceding December to April. The correlation co-

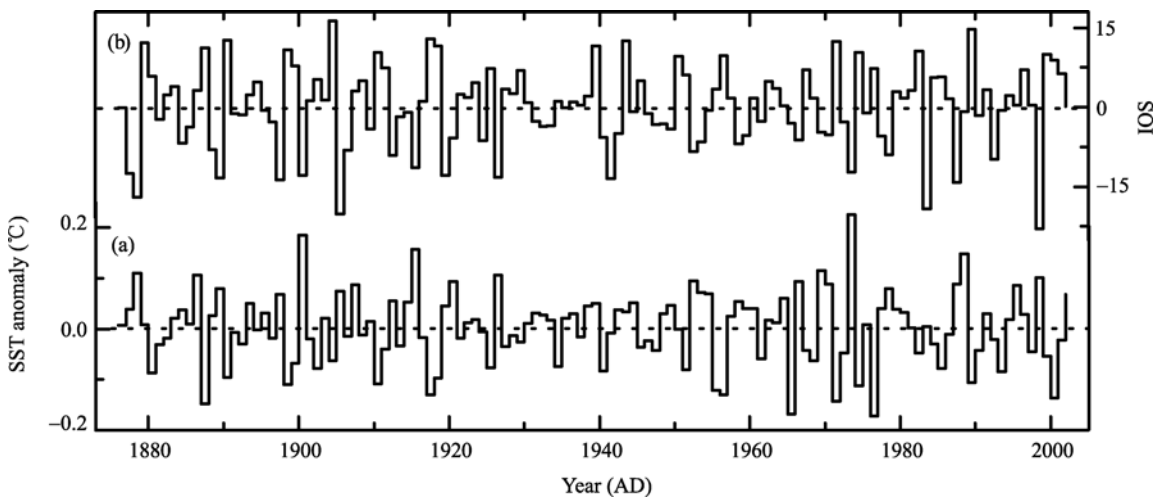

Figure 4 Comparison of the warm pool SST (a) with SOI (b).

efficients are –0.60 and –0.64 at observation period and reconstruction period respectively, both significant at the 0.01 level. The highly consistent relations between the observation and reconstruction period indicate that links between warm pool SST and ENSO variability are stable on interannual scale. At the same time, this also provides confidence to the reliability of the warm pool SST high-frequency reconstruction.

Regional temperature is usually influenced by large-scale climate background, and so are the long-term changes of warm pool SST. Comparison of warm pool SST with tropical regions SST and the whole tropical temperature are shown in Figure 5. Series (a) is March to July mean warm pool SST reconstruction for the 1644—1949, and shown together is the observed SST from HadISST data sets for the 1950—2006. Series (b) is the whole tropical sea temperature reconstructed by Wilson et al.[14]. Series (c) is the whole tropical mean temperature (combined land-surface air temperature and SST) based on HadCRUT3 from IPCC-AR4[39,40]. Generally, a good consistency among three series can be found in Figure 5. The correlation coefficient between the warm pool SST (a) and the whole tropical SST (b) is +0.59, and on interdecadal timescale they are correlated at +0.59, significant at the 0.01 level. However, there are notable differences during the period of 1790—1830. After 1830s, their correlations increase again (+0.81), significant at the 0.01 level. The correlation coefficient between the warm pool SST and the whole tropical temperature (c) is +0.73 during the 1950—2006 period, significant at the 0.01 level. In Figure 5, series (a) and series (c) present a good consistency in most of the time, e.g., from warm phase to cold phase and then to warm phase again during the period of the 1850s—1870s; cold/warm transition frequently and then from warm peak to cold valley rapidly during the period of 1896—1910; cold valley in 1955, 1956 and 1989; warm peak in 1975—1977, 1987, 1988 and 1998; all these changes are in good agreement. In the 1940s, all the three series have a warm peak. However, the peaks appear in slightly different times. The warm peaks of series (b) and (c) occur in 1940—1943, but for series (a) appears in 1942—1944. From the above analyses, we conclude that the coral proxies-based reconstruction of the warm pool SST is generally consistent with the whole tropical ocean SST and the whole tropical temperature, indicating that the warm pool SST variations are also affected by global climate change background, especially in low-frequency variations, e.g., the decadal variability. Meanwhile, there also exist some differences among the three temperature series. Part of these differences and uncertainties might arise from the differences in research area and temporal resolution. Furthermore, their difference may indicate the regional features of the warm pool SST.

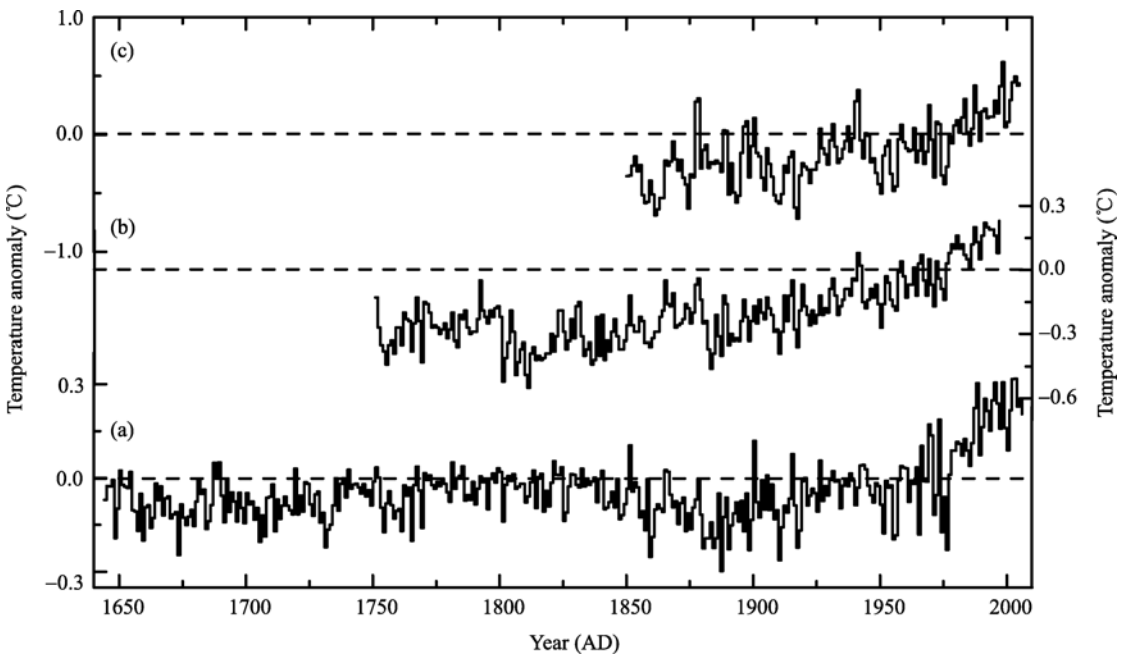

Figure 5 Comparison of raw-reconstruction SST (a) with the whole tropical SST (b) and the whole tropical temperature (combined land-surface air temperature and SST) from HadCRUT3 (c).

3 Comparison of historical warm pool SST with precipitation in East China

Modern meteorological data indicate that the western Pacific warm pool exerts an important influence on the subtropical high and the East Asian monsoon, and then could affect the temperature and precipitation variations in the most part of China. Huang at al.[41] has pointed out, when the western tropical Pacific warm pool (a relatively small area with a center in about 110°—140°E and 10°—20°N) is warmer than normal, the convective activities from around the Philippines to the Indo-China Peninsula through the South China Sea are intensified, the western Pacific subtropical high may shift northward, the summer rainfall tends to decrease in the Yangtze River basin and the Huaihe River basin. On the contrary, when the convective activities are weak there, the western Pacific subtropical high may shift southward, and the summer rainfall tends to increase in the Yangtze River basin and the Huaihe River basin and to decrease in the Yellow River basin and yield a drought summer there. The warm pool SST and East China precipitation anomalies are related through a teleconnection pattern in the atmospheric circulation anomalies over the regions from tropical East Asia to the middle latitudes, and even extending to the western coast of North America. In addition, Gong et al.[42] has pointed out, if the SST of the equatorial eastern Pacific in winter and that of the tropical western Pacific and the eastern Indian Ocean in summer is warmer than normal, the tropic monsoon will become weaker, and the subtropic monsoon will become stronger. The cold and warm airflow will converge in the Yangtze River basin and the Mei-yu front will be strengthened, then the rainfall of summer in Yangtze River basin will increase.

Above analyses are all based on the short, modern observation data, and it would be very interesting to see whether the relationship between the precipitation in East China and the western Pacific warm pool SST still exists during the historical periods. Here, we used the summer precipitation data collected at the 71 stations in China to analyze its relations to the warm pool SST. The summer precipitation data are reconstructed from historical documents or observations during 1880—1949 and updated using observational data for 1950—2005 period[43,44]. The results show that the correlations between the summer precipitation and the warm pool SST are positive for almost all stations in the south of the Yangtze River and negative for almost all stations in the north of the Yangtze River. There are thirteen stations with significant correlations ($r \leqslant -0.2$, significant at the 0.01 level) in the Yellow River basin and the Huaihe River basin (large circles in Figure 6). The mean series of thirteen sites is used as summer precipitation index for this region (Figure 7(c)) and compared with the warm pool SST (Figure 7(a)). The correlation coefficients between them are –0.46 in observation period and –0.44 in reconstruction period respectively, both significant at the 0.01 level. On interdecadal timescale, the warm pool SST can explain 72% and 67% variances of summer precipitation in observation and reconstruction periods respectively. The relation in reconstruction period is consistent with observation period, indicating the links between them are robust. In other words, when the warm pool is warmer than normal, the precipitation in the Yellow River basin and Huaihe River basin is usually below the normal. On the contrary, when the warm pool is colder than normal, precipitation tends to increase.

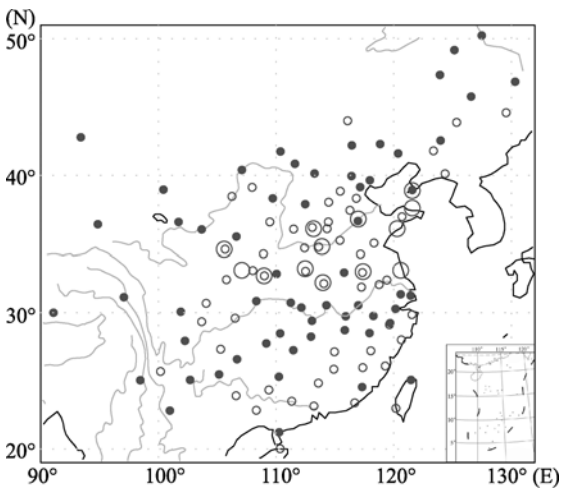

Figure 6 Correlation map of warm pool SST related to summer precipitation and flood-drought index in China. The solid dots represent positive correlations between the warm pool SST and the flood-drought index and the circles represent negative ones, the large circles represent the thirteen summer precipitation sites correlated significantly ($r \leqslant -0.2$, significant at the 0.01 level) with the warm pool SST.

In addition, based on 120 sites of flood-drought data from the refs. [45—47], we made a further analysis on the correlations between the warm pool SST and the precipitation in China. Because the flood-drought data before 1950 come from historical document records for

drought and flood events with yearly resolution, the flood-drought index is not as good as the summer precipitation data. Since rainfalls occur mainly in summer in the most part of China, the flood-drought index can generally well represent the summer precipitation. To facilitate comparison and reading, we standardize flood-drought data into 0－1, 0 for the most severe drought and 1 for the most severe flood. Correlations of the warm pool SST and the flood-drought index in China during the last 360 years are shown in Figure 6, solid dots for positive correlations and circles for negative correlations. The positive correlation means that the site is wetter than normal when the mean warm pool SST (March to July) is higher than normal, and negative correlation means that the site is drier than normal, respectively. In Figure 6, the distributions of positive and negative sites show obvious regional differences. In general, the positive and negative signs appear alternatively from northeast to southwest. The southeast coast is the negative correlation region, the lower Yangtze River basin to Yungui Plateau is the positive-dominated region, and then the positive signs appear in the Huaihe River basin to Yellow River basin, and again the positive-dominated condition takes place in Haihe River basin and regions north to it. Among these stations, the significant correlations are also located in the Yellow River basin and Huaihe River basin. We take the mean series of eight representative stations (all with $r \leqslant -0.2$, significant at the 0.01 level) as the flood-drought index for this region (Figure 7(b)). The correlation coefficients between them are –0.46 in observation period (1950－2000) and –0.20 in reconstruction period (1644－1949) respectively, and –0.24 for the whole period (1644－2000), all significant at the 0.01 level. The correlation is more obvious on interdecadal timescale; the correlation coefficient is –0.42 after low- pass filtered. On interdecadal timescale, the warm pool SST is correlated well with the flood-drought index. When the warm pool is warmer than normal, the Yellow River and Huaihe River basin are usually drier than normal, and when the warm pool is colder than normal, this region is usually wetter than normal. The drier periods, including 1658－1673, 1681－1698, 1715－1725, 1783－1793, 1802－1812,

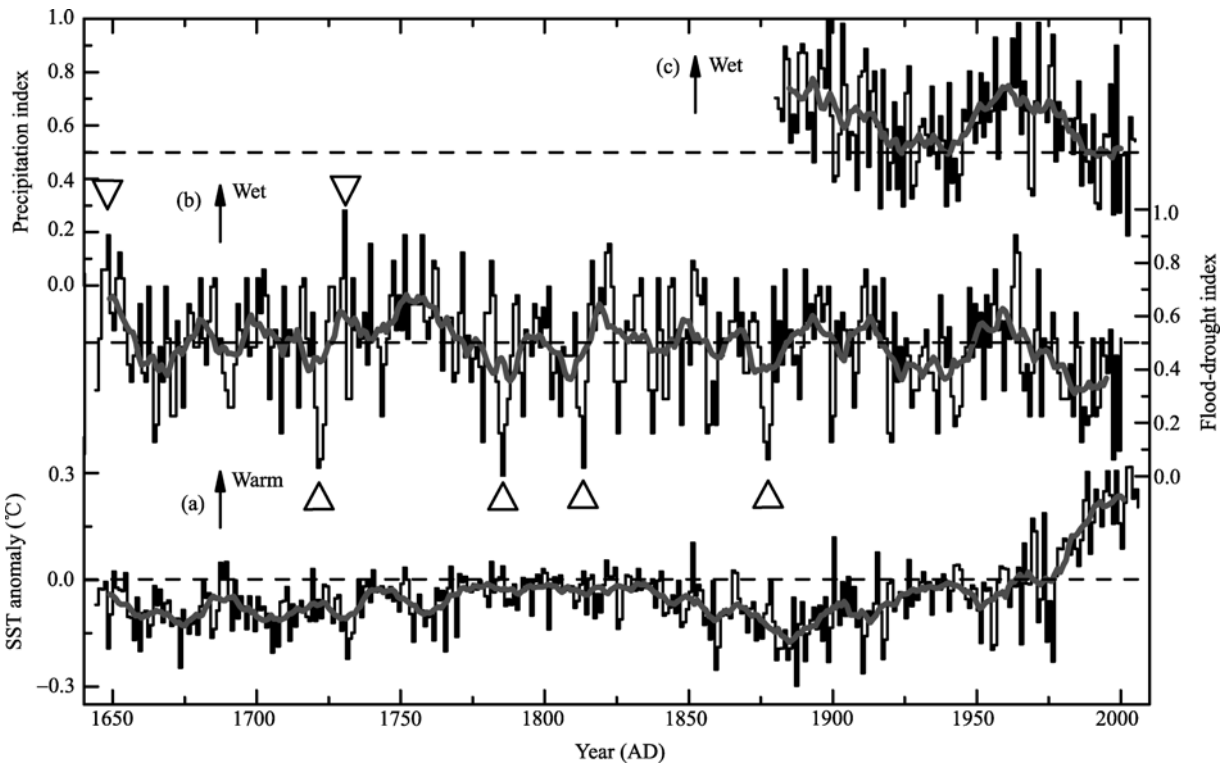

Figure 7 Comparison of the warm pool SST (a) with the flood-drought index (b) and the summer precipitation index (c) in the Yellow River basin and Huaihe River basin. Observation data for 1950－2006 and reconstruction for 1644－1949 are shown in series (a). The thick lines represent the 11-point moving average in series (a), (b) and (c). In series (b), Δ represent the flood-drought index below -2σ and ▽ represent the flood-drought index above $+2\sigma$ during the reconstruction period.

1870－1890, 1895－1910, 1915－1950 AD, correspond generally with warmer warm pool SST (except 1870－1890s). The obvious wetter period (1745－1775) corresponds to a lower warm pool SST. It should be noted that the warm pool SST keeps a stable warmer state during the period of 1780 － 1860. However, the flood-drought index shows large fluctuations during the same time period. On interannual timescale, their correlation is generally poor when checked year-to-year. Since 1960s the summer precipitation index and the flood-drought index both demonstrate obvious decreasing trends, corresponding with the increasing trend of the warm pool SST. This trend may be influenced by the background of global warming. On the longer low-frequency variations, Zhu at al.[48] pointed out there is a distinct 80a-oscillation of summer rainfall over North China, and this 80a-oscilla- tion basically agrees with the 80.7a long periods of the warm pool SST, suggesting the possible role of warm pool in the low-variability of East Asian summer monsoon climate.

Compared to interdecadal timescale, the interannual relations between the warm pool SST and precipitation over the Yellow River and Huaihe River basin are generally weaker. The high-frequency correlation coefficients between the warm pool SST and the summer precipitation index and the flood-drought index are –0.10, –0.13 in observation period and –0.26, –0.07 in reconstruction period, respectively. It indicates that the warm pool SST signals in the rainfalls over this area are weaker on interannual timescale. This may be related to the fact that there are many factors affecting the interannual rainfall fluctuations. It is interesting to note that some extreme flood events and drought events correspond well to warm pool SST anomalies during the reconstruction period (1644－1949). The four extreme drought years (flood-drought index anomalies $<-2\sigma$, including 1721, 1785, 1813 and 1877) correspond to the extremely high warm pool SST, and the two extreme flood years (flood-drought index anomalies $>2\sigma$, including 1648 and 1730) correspond to the extremely low warm pool SST (Figure 7). This shows that the anomalous warm pool SST may play an important role in the formation of extreme flood and drought events over the Yellow River and Huaihe River basin.

4 Conclusions

We statistically reconstructed the western Pacific warm pool SST back to 1644 using a coral proxy network in the western Pacific basin, and found skillful estimates for both the high and low frequency domains. Statistics (r^2, SE, RE) show that the reconstructed warm pool SSTs are reliable on the whole. The raw-reconstruction shows an obvious increasing trend of +0.04℃/100 a during the last 360 years, and three sub-stages are found existing significant linear trends, including the period 1644－1825 (+0.04℃/100 a), the period 1826－1885 (–0.24℃/100 a) and the period 1886 － 2006 (0.67 ℃/100 a). Power spectral analysis indicates that the significant leading periodicities are ~2.1, ~2.3, ~2.9, ~3.6, ~3.8 and 80.7-year during the last 360 years.

Correlations between the reconstructed warm pool SST and summer precipitation over East China show obvious regional features, significant and negative correlations appearing in the Yellow River and Huaihe River basin. The correlation coefficients between the warm pool SST and the regional summer precipitation index in this area during the observation period 1950－2005 and the reconstruction period 1880－1949 are –0.46 and –0.44, respectively, suggest a stable links between them. Their relationships are also significant during the last 360 years when checked with the historical flood-drought index. The correlation coefficients of the warm pool SST and the flood-drought index are –0.46 in the observation period (1950－2000) and –0.20 in the reconstruction period (1644－1949). On interdecadal timescale, they are correlated at –0.42, significant at the 0.01 level. The analysis shows that the warm pool SST is one of the important factors exerting influences on the summer precipitation in East China during the past 360 years, particularly on the decadal to interdecadal time scale. The reconstructed warm pool SSTs may provide some useful information and reference for climate change studies in East China.

Authors would like to sincerely thank three anonymous reviewers for valuable comments.

1 Nitta T. Convective activities in the tropical western Pacific and their impact on the northern hemisphere summer circulation. J Meteorol Soc Jpn, 1987, 65: 373－390

2 Huang R H, Li W J. Impacts of the abnormal thermal state over the

western pacific on the summer subtropical high over East Asia and its mechanism (in Chinese). Acta Meteorol Sin, 1987, (Special issue): 107－116
3 Zhao Z G. Summer Floods and Drought in China and Environmental Background (in Chinese). Beijing: Meteorological Press, 1999
4 Knutson D W, Buddemeier R W, Smith S V. Coral chronometers: Seasonal growth bands in Reef Corals. Science, 1972, 177(4045): 270－272[DOI]
5 Isdale P J, Stewart B J, Tickle K S, et al. Palaeohydrological variation in a tropical river catchment: A reconstruction using fluorescent bands in corals of the Great Barrier Reef, Australia. Holocene, 1998, 8(1): 1－8[DOI]
6 Urban F E, Cole J E, Overpeck J T. Influence of mean climate change on climate variability from a 155-year tropical Pacific coral record. Nature, 2000, 407(6807): 989－993[DOI]
7 Tudhope A W, Chilcott C P, McCulloch M T, et al. Variability in the El Niño-Southern Oscillation through a Glacial-Interglacial cycle. Science, 2001, 291: 1511－1517[DOI]
8 Cobb K M, Charles C D, Hunter D E. A central tropical Pacific coral demonstrates Pacific, Indian, and Atlantic decadal climate connections. Geophys Res Lett, 2001, 28(11): 2209－2212[DOI]
9 Fleitmann D, Burns S J, Ulrich N, et al. Palaeoclimatic interpretation of high-resolution oxygen isotope profiles derived from annually laminated speleothems from Southern Oman. Quat Sci Rev, 2004, 23(7-8): 935－945[DOI]
10 Guilderson T P, Schrag D P. Reliability of coral isotope records from the western Pacific warm pool: A comparison using age-optimized records. Paleoceanography, 1999, 14(4): 457－464[DOI]
11 Cole J E, Fairbanks R G, Shen G T. Recent variability in the Southern Oscillation: Isotopic results from a Tarawa Atoll coral. Science, 1993, 260(5115): 1790－1793[DOI]
12 Evans M N, Fairbanks R G., Rubenstone J L. A proxy index of ENSO teleconnections. Nature, 1998, 394(6695): 732－733[DOI]
13 McCulloch M, Fallon S, Wyndham T, et al. Coral record of increased sediment flux to the inner Great Barrier Reef since European settlement. Nature, 2003, 421(6924): 727－730[DOI]
14 Quinn T M, Crowley T J, Taylor F W. A multicentury stable isotope record from a New Caledonia coral: Interannual and decadal sea surface temperature variability in the southwest Pacific since 1657 AD. Paleoceanography, 1998, 13(4): 412－426[DOI]
15 Ryuji A, Tsutomu Y, Yasufumi I. Interannual and decadal variability of the western Pacific sea surface condition for the years 1787－2000: Reconstruction based on stable isotope record from a Guam coral. J Geophys Res, 2005, 110[DOI]
16 Evans M N, Kaplan A, Cane M A. Pacific sea surface temperature field reconstruction from coral δ^{18}O data using reduced space objective analysis. Paleoceanography, 2002, 17(1)[DOI]
17 Wilson R, Tudhope A, Brohan P. Two-hundred-fifty years of reconstructed and modeled tropical temperatures. J Geophys Res, 2006, 111[DOI]
18 Huang R H, Sun F Y. Impact of the convective activities over the western tropical Pacific warm pool on the intraseasonal variability of the East Asian summer monsoon (in Chinese). Sci Meteorol Sin, 1994, 18(4): 456－465
19 Zhang Q L, Weng X C, Yan T Z. Spatial and temporal variations of SST field in the western Pacific warm pool area (in Chinese). Oceanol Limnol Sin, 2001, 32(4): 349－354
20 Jin Z H, Chen J. A composite study of the influence of SST warm anomalies over the western Pacific warm pool on Asian summer monsoon (in Chinese). Chin J Atmos Sci, 2002, 26(1): 57－68
21 Zhang Z X, Liu X F, Teng D G. Spatial/Temporal features of SSTA in the western Pacific warm pool region and its relations to general circulation (in Chinese). J Nanjing Inst Meteorol, 2005, 28(6): 746－754
22 McPhaden M J, Picaut J. El Niño-Southern Oscillation displacements of the western equatorial Pacific warm pool. Science, 1990, 250(4986): 1385－1388[DOI]
23 Li K R, Zhou C P, Sha W Y. Basic features of the warm pool in the western Pacific and its impact on climate (in Chinese). Acta Geogr Sin, 1998, 53(6): 511－519
24 Zhao Y P, Wu A M, Chen Y L, et al. The climatic jump of the western Pacific warm pool and its climatic effects (in Chinese). J Trop Meteorol, 2002, 18(4): 317－326
25 Wyrtki K. Some Thought about the West Pacific Warm Pool. Proceeding of the Western Pacific International Meeting and Workshop on TOGA-COARE. New Caledonia: France Institute of the Scientific Research for the Development on the Cooperation, 1989. 99－109
26 Wang C, Enfield D B. The tropical western hemisphere warm pool. Geophys Res Lett, 2001, 28(8): 1635－1638[DOI]
27 Enfield D B, Sang-Ki L, Wang C Z. How are large western hemisphere warm pools formed? Progr Oceanogr, 2006, 70: 346－365[DOI]
28 Qiu D X, Huang F, Yang Y X. Interdecadal variability of the Indo-Pacific warm pool (in Chinese). Period Ocean Univ China, 2007, 37(4): 525－532
29 Rayner N A, Parker D E, Horton E B, et al. Global analyses of sea surface temperature, sea ice, and night marine air temperature since the late nineteenth century. J Geophys Res, 2003, 108: D14[DOI]
30 Smith T M, Reynolds R W. Extended reconstruction of global sea surface temperatures based on COADS data (1854－1997). J Clim, 2003, 16(10): 1495－1510
31 Gong D Y, Luterbacher J. Variability of the low-level cross-equatorial jet of the western Indian Ocean since 1660 as derived from the coral proxies. Geophys Res Lett, 2008, 35[DOI]
32 Lough J M. A strategy to improve the contribution of coral data to high-resolution paleoclimatology. Paleogeogr Paleoclimatol Paleoecol, 2004, 204(1-2): 115－143[DOI]
33 Lorenz E N. Empirical orthogonal functions and statistical weather prediction. Statistical Forecasting Project Report No 1. Boston: Dept of Meteor MIT, 1956. 49
34 Fritts H C. Tree Rings and Climate. London: Academic Press, 1976
35 Cook E R, Kairiukstis L A. Methods of Dendrochronology: Applications in the Environmental Sciences. New York: Springer, 1990
36 Cook E R, Briffa K R, Jones P D. Spatial regression methods in dendroclimatology: A review and comparison of two techniques. Int J Climatol, 1994, 14: 379－402[DOI]
37 Zhou T J, Yu R C, Li W, et al. On the variability of the Indian Ocean

during the 20th century (in Chinese). Acta Meteorol Sin, 2001, 59(3): 257－270
38 Wang S W, Zhu J H, Cai J N, et al. Reconstruction and analysis of time series of ENSO for the last 500 years (in Chinese). Prog Nat Sci, 2004, 14(4): 424－430
39 IPCC. Climate Change 2007: The Physical Science Basis. New York: Cambridge University Press, 2007. 237－336
40 Brohan P, Kennedy J J, Harris I, et al. Uncertainty estimates in regional and global observed temperature changes: A new dataset from 1850. J Geophys Res, 2006, 111: D12106, doi: 10.1029/2005JD006548
41 Huang R H, Sun F Y. Impacts of the thermal state and the convective activities in the tropical western warm pool on the summer climate anomalies in East Asia (in Chinese). Sci Atmos Sin, 1994, 18(2): 141－151
42 Gong Z S, He M. Relationship between summer rainfall in Changjang River valley and SSTA of various seasons (in Chinese). Meteorol Mon, 2006, 32(1): 56－61
43 Li Z H, Zhu J H, Cai J N, et al. Flood in Huaihe valley (in Chinese). Meteorol Mon, 2005, 31(6): 24－28
44 Wang S W, Gong D Y, Ye J L, et al. Seasonal precipitation series of Eastern China since 1880 and the variability (in Chinese). Acta Geogr Sin, 2000, 55(3): 281－293
45 Central Meteorological Bureau of China. Atlas of the Drought /Food Category for the Last 500 Years in China (in Chinese). Beijing: Map Press, 1981. 1－332
46 Zhang D E, Liu C Z. Continuation (1980－1992) of the "Atlas of the Drought /Flood Category for the Last 500 Years in China" (in Chinese). Meteorol Mon, 1993, 19(11): 41－45
47 Zhang D E, Li X Q, Liang Y Y. Re-continuation (1993－2000) of the "Atlas of the Drought /Flood Category for the Last 500 Years in China" (in Chinese). J Appl Meteorol Sci, 2003, 14(3): 379－388
48 Zhu J H, Wang S W. 80a-oscillation of summer rainfall over the east part of China and East-Asian summer monsoon. Adv Atmos Sci, 2001, 18(5): 1043－1050